Received: 15 December 2019 | Revised: 20 July 2020 | Accepted: 26 August 2020

DOI: 10.1002/term.3123

WILEY

RESEARCH ARTICLE

Peptide-mediated surface coatings for the release of wound-healing cytokines

Franziska Clauder[1] | Stephanie Möller[2] | Sebastian Köhling[3] | Kathrin Bellmann-Sickert[1] | Jörg Rademann[3] | Matthias Schnabelrauch[2] | Annette G. Beck-Sickinger[1]

[1]Institute of Biochemistry, Faculty of Life Sciences, Leipzig University, Leipzig, Germany

[2]Biomaterials Department, INNOVENT e.V., Jena, Germany

[3]Institute of Pharmacy, Medicinal Chemistry, Freie Universität Berlin, Berlin, Germany

Correspondence
Annette G. Beck-Sickinger, Institute of Biochemistry, Faculty of Life Sciences, Leipzig University, Brüderstrasse 34, 04103 Leipzig, Germany.
Email: abeck-sickinger@uni-leipzig.de

Funding information
Deutsche Forschungsgemeinschaft, Grant/Award Numbers: TRR 67 projects A04, A08, Z03, Z03, A08, A04, TR67; Research Academy Leipzig; Adipositas and Vascular Research (HI-MAG); Helmholtz-Institute for Metabolism; European Union and the Free State of Saxony

Abstract

Supporting the wound healing process by sending the appropriate cytokine signals can shorten healing time and overcome chronic inflammation syndromes. Even though adhesion peptides consisting of Arg-Gly-Asp (RGD) are commonly used to enhance cell-surface interactions, peptide-mediated cytokine delivery has not been widely exploited so far. Cytokines interact with high affinity with their cognitive receptors but also with sulfated glycosaminoglycans (GAGs), both of which form a base for incorporation of cytokines into functional biomaterials. Here, we report on a mussel-derived surface coating as a prospective cytokine delivery system using covalently bound heparin mimetics, receptor-derived chemokine-binding peptides, and heparin-binding peptides (HBP). The latter enabled non-covalent immobilization of heparin on the surface followed by chemokine binding and release, whereas the former allowed direct non-covalent chemokine immobilization. The peptide displayed excellent binding to custom-made polystyrene 96-well plates, enabling convenient testing of several compounds. Released chemokine successfully induced migration in Jurkat cells, especially for the non-covalent heparin immobilization approach using HBPs as evaluated in a transwell assay. In comparison, heparin-mimetic coatings, comprised of sulfated peptides and GAG derivatives, proved less efficient with respect to amount of immobilized chemokine and migratory response. Thus, our study provides a roadmap for further rational optimization and translation into clinics.

KEYWORDS

cell migration, DOPA, drug delivery system, heparin, surface-coated materials, wound healing

1 | INTRODUCTION

Chemokines are a family of small 8–12 kDa proteins that mediate migration and arrest of their target cells. They are crucial players in tissue regeneration as they orchestrate the recruitment of various cell types to the wound site, modulating the immune response and directing angiogenesis. CXC chemokine ligand 12 (CXCL12) or stromal cell-derived factor 1α (SDF-1α) is a pleiotropic cytokine that signals through its G protein-coupled receptors CXCR4 and CXCR7 and acts as a chemoattractant. In adult organisms, CXCL12 promotes

angiogenesis, the recruitment of hematopoietic stem and progenitor cells, immune cell trafficking, and neuronal regeneration (Guyon, 2014; Liekens, Schols, & Hatse, 2010). Thus, the chemokine is involved in various stages of wound healing including homeostasis, inflammation, and proliferation (Ratajczak et al., 2006), making it an appealing component of biomaterials in tissue engineering. However, the development of suitable delivery strategies remains an ongoing field of research. Simple adsorption to the material already promotes tissue regeneration (Ji et al., 2013), but stabilization against rapid protein clearance and a controlled release to reduce side effects is desirable. In opposition, covalent immobilization approaches require protein engineering to incorporate functional groups for surface binding and cleavable linkers for protein release (Steinhagen et al., 2014), which can alter protein activity. Thus, affinity-based delivery systems are to be exploited, where a binding ligand is immobilized to the material, which then reversibly binds the unmodified chemokine.

In the extracellular matrix, glycosaminoglycans (GAGs) like heparin and heparan sulfate represent the most important binding partners of CXCL12. Stabilization by GAGs is essential for the formation of chemotactic gradients and protects the chemokine from inactivating posttranslational modifications (Janssens, Struyf, & Proost, 2018). This heparin-binding affinity can be exploited for the delivery by covalent or non-covalent incorporation of heparin into biomaterials (Vulic & Shoichet, 2014). Heparin-binding peptides (HBPs) contain a number of basic residues to interact with the negatively charged GAGs and therefore offer the possibility to immobilize heparin by electrostatic interaction (Cardin & Weintraub, 1989; Sakiyama-Elbert & Hubbell, 2000). In these cases, the cytokine as well as the mediating GAG will be released over time. Specifically functionalized heparin or heparin analogs can mediate orthogonal conjugation to the material. Sulfated hyaluronic acid (sHA) derivatives have been developed as heparin-like protein-binding polymers that, when applied as high molecular weight sHA or even as short oligomeric compounds, have proven to bind CXCL12 (Köhling et al., 2019; Purcell et al., 2014). Another possibility is the complete replacement of the sugar with peptidic compounds. However, for explicit delivery of CXCL12, only receptor-derived peptides (RDPs) are known so far (Peled, Eizenberg, & Vaizel-Ohayon, 2012), some of which include also posttranslational tyrosine sulfation (Veldkamp, Seibert, Peterson, Sakmar, & Volkman, 2006). For the delivery of other cytokines, a number of heparin-mimetic peptides (HMPs) are known. Sulfates are included either by O-sulfation of serine and threonine residues or by incorporation of sulfotyrosines. Maynard and Hubbell identified the consensus sequence SY*DY*G, where Y* is a sulfotyrosine, which was confirmed to bind vascular endothelial growth factor (VEGF; Maynard & Hubbell, 2005), transforming growth factor β, and bone morphogenetic protein 4 (Hendrikse, Spaans, Meijer, & Dankers, 2018). Within another approach, sulfobenzoic acid (sba) is coupled to lysine side chains to incorporate sulfate groups into a molecular brush (Mammadov et al., 2011). The peptide EGDK(sba)S was shown to bind VEGF, hepatocyte growth factor, and fibroblast growth factor 2 (Mammadov, Mammadov, Guler, & Tekinay, 2012) to enhance angiogenesis and wound healing.

Within the present study, affinity-based delivery strategies for CXCL12 inspired by extracellular matrix-proteoglycan interactions were investigated. Here, functional peptide coatings were used to immobilize GAGs and GAG mimetics onto a polymer surface in order to provide a prospective chemokine delivery system that is easily prepared, purified, and analyzed. This was enabled by incorporation of L-3,4-dihydroxyphenylalanine (DOPA), a nonproteinogenic amino acid identified in the byssus of blue mussels (Waite & Tanzer, 1981), into surface-binding peptides. In this work, application of the catechol-based coating was shown to go beyond metal oxide surfaces, where display of cell adhesives promoted osseointegration and endothelialization (Clauder et al., 2019; Pagel et al., 2016). Using the peptide as a modifiable anchor provided a platform to compare HBPs, subsequently loaded with heparin, sHA derivatives, and sulfated peptides but also receptor-derived chemokine-binding peptides for CXCL12 binding. Finally, gradient formation was investigated by transwell migration studies to test for effective cell recruitment.

2 | MATERIALS AND METHODS

2.1 | Chemicals

Fluorenylmethoxycarbonyl (Fmoc)–protected amino acids, resins, and coupling reagents were purchased from IRIS Biotech. *N*,*N*-dimethylformamide (DMF), dichloromethane (DCM), and N-methyl-2-pyrrolidon (NMP) were purchased from Biosolve, whereas acetonitrile (ACN) was obtained from VWR. Hyaluronic acid (HA, from *Streptococcus*, MW = 1,100 kDa) was obtained from Aqua Biochem. Sulfo-N-succinimidyl 4-maleimidobutyrate (XLINK) was from Bachem, and monomeric avidin agarose beads was from Pierce. Tris (hydroxymethyl)aminomethane (Tris) and bovine serum albumin (BSA) were obtained from Roth, and antibodies from Santa Cruz Biotechnology, Inc. 3,3′,5,5′-Tetramethylbenzidine (TMB) was from Merck and HCl from Grüssing. RPMI 1640 was purchased from Lonza and fetal calf serum (FCS) from Biochrome. All other reagents were obtained from Sigma-Aldrich.

2.2 | Peptide synthesis

All peptides were synthesized by a combination of manual couplings and automated solid-phase peptide synthesis using a Syro I peptide synthesizer (MultiSynTech) under standard Fmoc/tert-butyl (tBu) conditions. The N_α-Fmoc-deprotection was achieved with piperidine in DMF, and amino acids were activated with equimolar amounts of *N*,*N*-diisopropylcarbodiimide (DIC) and 1-hydroxybenzotriazole (HOBt) or hydroxyiminocyanessigsäureethylester (oxyma), respectively. The peptides HBP-N_3 and HBP_2-N_3 were produced in the synthesizer on Rink amide resin and N-terminally modified with ε-azido-L-lysine. Heparin-mimetic peptide 1 (HMP1) and HMP2 as well as motif repetitions were likewise produced automatically, whereby Fmoc-L-Lys(Dde)-OH was incorporated at future sulfation

sites. After N-terminal trityl-protection or acetylation, selective deprotection of the lysine side chain was achieved with 3% hydrazine in DMF. sba was coupled in two-fold excess with equimolar amounts of 1-[bis (dimethylamino)methylene]-1H-1,2,3-triazolo[4,5-b] pyridinium 3-oxide hexafluorophosphate and one equivalent N,N-diisopropylethylamine overnight. RDP was likewise produced automatically on Rink amide resin. The mussel-derived peptide (MP) derivatives were analogously synthesized as described elsewhere (Pagel et al., 2016). MP(+) and MP(–) were produced by elongation with Fmoc-L-aminohexanoic acid and subsequently biotinylated with HOBt/DIC in NMP. Conjugation of MP with the HBPs HBP-N_3 and HBP_2-N_3 by Cu(I)–catalyzed azide alkine cycloaddition was likewise performed as described by Pagel et al. (Pagel et al., 2016). Thiol- and maleimide-functionalized compounds were combined by Michael addition reaction, which was carried out for at least 2 h in degassed sodium phosphate buffer pH 6.8. Successful conjugation was observed by a retention time shift during reversed-phase high-performance liquid chromatography (RP-HPLC) analysis, whereby in all cases, less than 2% unfunctionalized MP remained.

2.3 | Full cleavage and peptide purification

Full cleavage of the peptides was achieved by incubation with a mixture of trifluoroacetic acid (TFA) and scavenger for 3 h at room temperature, shaking. For HBPs, 90% TFA and 10% water was used. The sulfated peptides were cleaved using 95% TFA and 5% triisopropyl silane/water (1:1, *v*/v). RDP was cleaved with 90% TFA and 10% thioanisole/ethanedithiole (7:3, *v*/v). Peptides were precipitated and washed with ice-cold diethyl ether. Peptide purification was carried out by preparative RP-HPLC on a Phenomenex Kinetex XB-C18 column (100 Å, 5 μm, 250 × 21.2 mm) using linear gradients of Eluent B in Eluent A (A: 0.1% TFA in water; B: 0.08% TFA in ACN). Analytical identification of the peptides was performed by matrix-assisted laser desorption/ionization time of flight mass spectrometry (MALDI-ToF-MS; Bruker Daltonics) and electrospray ionization-Ion Trap MS (Bruker Daltonics), and observed m/z values matched the calculated molecular weights. Final purity was confirmed by analytical RP-HPLC on two of the three following columns: Phenomenex Jupiter Proteo column (90 Å, 4 μm), Agilent Technologies VariTide RPC column (200 Å, 6 μm), or Phenomenex Jupiter C18 column (300 Å, 5.3 μ) using linear gradients of Eluent B in Eluent A.

2.4 | Synthesis of sulfated GAG derivatives and coupling to MP

The fully sulfated nonasulfo-tetrahyaluronan-polyethylene glycol (PEG)-thiol (sHA1) was obtained by tris-(2-carboxyethyl)-phosphane (TCEP)–mediated reduction of the bivalent octadeca-sulfo-disulfide (9s-HA-4-S-PEG-S-)$_2$ that was synthesized as reported previously (Köhling et al., 2019). The disulfide reduction was performed as follows: 2,3,4,6-tetra-O-sulfo-β-D-glucopyranuronyl-(1 → 3)-4,6-di-O-sulfo-β-D-2-acetamido-2-deoxy-glucopyranosyl-(1 → 4)-2,3-di-O-sulfo-β-D-glucopyranuronyl-(1 → 3)-4,6-di-O-sulfo-β-D-2-acetamido-2-deoxy-glucopyranosyl-1-thio-2-ethyloxy-2-ethylox-2-ethyl-disulfide, (9s-HA-4-S-PEG-S)$_2$ (49 mg, 12.6 μmol) was dissolved in 2 ml of degassed phosphate buffered saline (PBS; 0.2 M, pH: 7.5) and stirred under argon atmosphere. TCEP (9 mg, 31.6 μmol) was added and the reaction mixture was stirred for 5 min at room temperature. Subsequently, the mixture was transferred into a dialysis tube (cellulose acetate, molecular weight cut-off = 1,000 Da) and excessively dialyzed against degassed water for 1 day. The product was transferred from the dialysis tube into a flask and freeze-dried to yield sHA1 as a white powder (47 mg, 96%). **^{1}H NMR** (700 MHz, D_2O) δ [ppm] = 5.18 (d, *J* = 4.1 Hz, 1H), 5.06–5.03 (m, 2H), 4.93 (d, *J* = 6.7 Hz, 1H), 4.87–4.83 (m, 2H), 4.79 (d, *J* = 10.4 Hz, 1H), 4.56 (dd, *J* = 11.4, 2.2 Hz, 1H), 4.55–4.52 (m, 2H), 4.47 (t, *J* = 4.3 Hz, 1H), 4.43 (d, *J* = 6.7 Hz, 1H), 4.39 (dd, *J* = 6.7, 2.6 Hz, 1H), 4.30 (t, *J* = 9.4 Hz, 1H), 4.27 (t, *J* = 9.2 Hz, 1H), 4.23–4.15 (m, 3H), 4.08 (dd, *J* = 11.5, 7.9 Hz, 1H), 4.00 (t, *J* = 9.3 Hz, 1H), 3.91–3.86 (m, 3H), 3.82 (s, 1H), 3.77–3.70 (m, 2H), 3.70–3.63 (m, 6H), 2.93 (dt, *J* = 13.6, 6.6 Hz, 1H), 2.84 (dt, *J* = 14.1, 6.3 Hz, 1H), 2.69 (t, *J* = 6.3 Hz, 2H), 2.11 (s, 3H), 2.07 (s, 3H).; **^{13}C NMR** (176 MHz, D_2O) δ [ppm] = 174.72, 174.51, 174.04, 100.75, 100.09, 99.48, 84.79, 79.76, 79.04, 78.84, 78.05, 77.97, 77.23, 76.87, 76.59, 75.61, 75.40, 74.87, 72.92, 72.23, 70.17, 69.51, 69.22, 67.93, 67.59, 55.77, 54.56, 30.28, 28.14, 23.22, 22.99, and 22.77. Coupling to MP-Male was performed as described for the sulfated peptides and monitored by RP-HPLC.

Low-molecular-weight HA samples (HA1, M_W = 43 kDa, and HA2, M_W = 115 kDa) were prepared by thermal degradation of HA in an autoclave according to a published protocol (Kunze et al., 2010). The sulfated polymer derivatives sHA2 and sHA3 were synthesized by sulfation of the degraded HA1 and HA2 samples with SO_3-pyridine (OH/SO_3 = 1:15) for sHA2 and SO_3-DMF (OH/SO_3 = 1:20) for sHA3, respectively. Introduction of amino groups proceeded by reductive amination with ethylendiamine dihydrochloride (EDA × 2 HCl) and $NaCNBH_3$ as follows: a 10 mg/ml aqueous solution of sHA was saturated with EDA × 2 HCl over several hours. After pH adjustment to 7.4, $NaCNBH_3$ was added and the mixture stirred for 3 days. Subsequently, the solution was dialyzed against 0.125 M aqueous $NaHCO_3$-solution for further 3 days following dialysis against water. The final products were lyophilized and dried. The contents of amino groups were determined by Kaiser test. Analytical data of the prepared GAG derivatives are summarized in Table S2. Amine-functionalized sHA derivatives were initially reacted with 5 eq XLINK in 10 mM sodium phosphate buffer pH 8 at 4°C overnight. After size exclusion centrifugation (7,500 g, 15 min) with a cut-off at 10 and 30 kDa, respectively, to separate unreacted crosslinker, the compounds were subsequently coupled with 5 eq biotinylated (Bio)-MP(Ala) by Michael addition reaction as described above. Excess Bio-MP(Ala) was again removed by size exclusion chromatography. The orthogonality of the reaction was monitored on a Varian Cary® 50 UV–Vis Spectrophotometer measuring the absorption spectrum between

200 and 300 nm. The amount of peptide was determined via the absorption of the DOPA units at 280 nm and a linear standard curve obtained from MP (r^2 = 0.99). Finally, MP-XLINK-sHA2/3 were purified using affinity chromatography. Monomeric avidin agarose beads were washed and loaded with the reaction mixture as described in the manufacturer's protocol. Finally, peptide-crosslinked GAG were eluted using 2 mM biotin in PBS.

2.5 | Peptide immobilization

Serial dilutions of MP(+) and MP(–) in 10 mM Tris buffer pH 7.6 were incubated in polystyrene 96-well plates overnight at room temperature and shaking. Afterwards, unbound peptide was washed off with tris-buffered saline-tween20 (TBS-T; 50 mM Tris, 150 mM NaCl, 0.1% tween20, pH 7.6). Detection of bound MP was performed via the biotin tag in an enzyme-linked immunosorbent assay (ELISA)–like assay, as described previously (Hassert et al., 2012). The experiment was performed three times in triplicates, and data are shown as mean ± standard error of the mean (sem).

For further investigations, a 1 μM peptide dilution in 10 mM Tris buffer pH 7.6 was incubated on the microtiterplate overnight. After washing with TBS-T, incubation with heparin and/or CXCL12 continued.

2.6 | Heparin binding

MP-HBP and MP-HBP_2 were immobilized onto 96-well plates overnight. Subsequently, wells were incubated with 1 μM biotinylated porcine heparin (bio-Hep, M_W = 15 kDa, DS = 1.8–2.2) in TBS buffer (50 mM Tris, 150 mM NaCl, pH 7.6, 8.3 or 8.9) for 1 h. Detection occurred via the biotin tag as described above. The data are derived from at least three independent experiments performed in triplicates and displayed as mean + sem.

2.7 | CXCL12 binding

Full-length CXCL12, carrying a C-terminal methionine due to *Escherichia coli* expression, was produced, refolded, and purified as described previously (Spiller et al., 2019). Peptides were immobilized and subsequently loaded with 1 μM heparin (M_W = 15 kDa, DS = 1.8–2.2) for 1 h and 1 μM CXCL12 for 2 h. After another washing step with TBS-T, wells were blocked with 10% BSA in TBS and bound CXCL12 was detected using mouse-anti-SDF-1 (1:500 in 1% BSA in TBS) and goat-anti-mouse-IgG-horseradish peroxidase (HRP; 1:5,000 in TBS). Addition of the peroxidase substrate TMB and halting the conversion after 5 min with 1 M HCl enabled quantitative readout at 450 nm absorption (infinite M200, Tecan). The experiment was performed at last twice in triplicates. Data are normalized to MP-HBP = 1 and represented as mean + sem.

2.8 | Migration

The lower chambers of a 96-well high throughput screening transwell plate (5 μM pore size, Corning) were coated with peptide, heparin, and CXCL12, as described earlier. Rinsing several times with PBS removed remaining TBS-T from the washing steps. Jurkat cells (kindly gifted by the Institute of Immunology, University Hospital Leipzig) were kept in RPMI 1640 with 10% FCS at 37°C in a humidified atmosphere containing 5% CO_2. For migration assays, cells were spun down and resuspended in RPMI 1640 containing 2% FCS (migration media). 4×10^5 cells per 100 μl were loaded to the upper chambers. The lower chambers were filled with 250 μl migration media, and 50 nM CXCL12 were used as positive control. After incubation at 37°C for 2 h, 100 μl sample per well was mixed with 100 μl 0.5% trypan blue in PBS. The number of migrated cells was determined at a Spark plate reader (Tecan) using the automatic cell-counting application (Cell Chip). Data were obtained from at least three independent experiments performed in duplicates and is shown as mean + sem.

2.9 | Statistical analysis

Statistical analysis was implemented with Prism 5.0 (GraphPad), and significances were determined with one-way ANOVA followed by Newman–Keuls multiple comparison test, except for surface binding studies, where a two-way ANOVA following Bonferroni posttests was applied.

3 | RESULTS

3.1 | DOPA-containing peptides efficiently coat polystyrene surfaces

Wound healing and regeneration are very complex and highly orchestrated processes. Numerous cell types are involved, whose function and timing are of utmost importance. Herein, cytokines execute important messenger functions, enabling the communication that regulates inflammatory processes, cell migration, cell activation, and cell survival. Releasing CXCL12 into acute or chronic wounds might help improve healing times due to its beneficial effect on revascularization and modulating role in immune cell recruitment. In our approach, we used a peptide derived from the marine blue mussel (MP) as a platform for presenting heparin-binding/mimetic sequences that allow sequestration of the chemokine from a solid support (Figure 1a). DOPA was incorporated for immobilization on polystyrene surfaces (PS), whereas orthogonal reaction groups enabled modification with peptides and GAGs. An N-terminally biotin-tagged derivative, termed MP(+), allowed detection of immobilized peptide with horseradish peroxidase-conjugated streptavidin (Strep-POD). In the control peptide MP(–), DOPA was replaced with tyrosine. Concluding from an ELISA-like assay, DOPA generally enhanced the amount of immobilized peptide to standard 96-well PSs in comparison

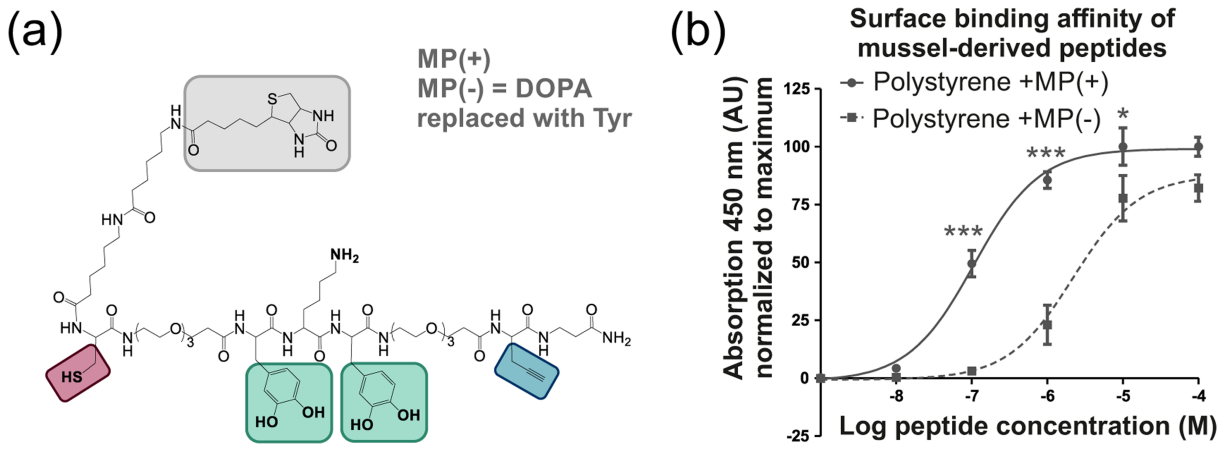

FIGURE 1 (a) Chemical structure of mussel-derived peptide (MP(+)). The L-3,4-dihydroxyphenylalanine (DOPA) units for surface binding are highlighted in green, and the biotin-tag for detection in gray. Functional groups for peptide conjugation by thiol-maleimide Michael addition reaction and Cu(I)-catalyzed azide-alkine cycloaddition (CuAAC) are highlighted in red and blue, respectively. (b) Surface binding of the mussel-derived anchor peptide MP(+) to polystyrene. MP(−), a tyrosine-containing peptide analog, shows a 20-fold loss in affinity in comparison to the DOPA-containing derivative. $n = 3$, $^{*}p \leq 0.05$, $^{***}p \leq 0.001$ with respect to MP(−) [Colour figure can be viewed at wileyonlinelibrary.com]

with the control peptide. A binding affinity study revealed a 20-fold shift in EC_{50} between the peptides (Figure 1b).

3.2 | Functional click chemistry enables the generation of heparin-binding and heparin-mimetic coatings

The two approaches described in this study based on cytokine-GAG-interactions to deliver CXCL12 from a peptidic surface coating are displayed schematically in Figure 2. On the one hand, a HBP coating electrostatically immobilizes heparin and subsequently delivers heparin-binding cytokines (Figure 2a, left). On the other hand, HMPs and sulfated GAG derivatives were covalently coupled to bind and release heparin-binding cytokines (Figure 2b, left). Although the DOPA units of MP anchor the coating to the surface, modification with functional peptides, GAGs, or GAG mimetics was achieved by introduction of orthogonal reaction groups. To enable the non-covalent immobilization of heparin, the HBPs HBP and HBP_2 were coupled to propargylglycine by Cu(I)-catalyzed azide-alkine cycloaddition (Figure 2a, middle). To investigate heparin binding, a biotinylated heparin derivative was incubated on MP-HBP- and MP-HBP_2-coated surfaces, respectively, and detected by Strep-POD (Figure 2a, right). Both peptides were found to efficiently immobilize heparin in comparison to unfunctionalized MP, whereby the elongated sequence HBP_2 gave a 2.8-fold higher signal than the single motif HBP. This loading efficiency was also observed when tested at basic conditions, as chronic wounds can have pH values up to 8.9 (Figure S1; Tsukada, Tokunaga, Iwama, & Mishima, 1979; Wilson, Henry, Quill, & Byrne, 1979).

In comparison with the dual-affinity approach, which combines HBP and heparin for CXCL12 release, heparin-mimetic coatings were synthesized (Figure 2b). These coatings comprise small peptides as well as short and long sHA derivatives. For the generation of sulfated peptides, sba was coupled to lysine side chains of the sequence EGDKS, similar to a procedure reported by Mammadov et al. (Mammadov et al., 2011). This gave stable compounds that retained sulfation even under highly acidic conditions as during deprotection, full cleavage, and preparative HPLC. In contrast, direct incorporation of sulfotyrosine into the growth factor-binding sequence SYDYG proved to be too acid labile, especially when more than one sulfate group was incorporated. Accordingly, these residues were replaced with lysine and the peptide was analogously sulfated using sba (Figure 2b, right). During conjugation to MP-Male by thiol-maleimide Michael addition reaction (Figure 3a), an excess of sulfated peptide quantitatively consumed the MP. Thereby, less than 2% unmodified peptide remained, as monitored by RP-HPLC. A list of all synthesized precursor peptides and conjugates as well as analytical characterization is displayed in Table S1.

Beyond the synthesis of sulfated peptides, HA derivatives of differing size were tested: a fully synthetic nonasulfated tetrasaccharide (sHA1) and two chemically sHA derivatives of lower (sHA2) and slightly higher molecular weight (sHA3; Figure 2b, bottom). Although the short tetrasaccharide was equipped with a thiol functionality that enabled conjugation to MP-Male analogously to the sulfated peptides (Figure 3a), sHA2 and sHA3 displayed an ethylene diamine group at the reducing end. A crosslinker (XLINK) enabled conjugation to MP (Figure 3b). To prevent unspecific crosslinking, the surface-binding peptide was depleted of its lysine residue (MP(Ala)) and additionally equipped with a biotin-tag (Bio-MP(Ala)) for subsequent purification by monomeric avidin affinity chromatography. To verify whether the conjugation reaction was indeed specific, sHA2/3 and the MP were incubated with or without preceding XLINK conjugation. Absorption spectra of the reaction mixtures were recorded, whereby the absorption at 280 nm correlates to the DOPA residues within the peptide (Figure; 4a). In the sample without XLINK, only a small amount of peptide

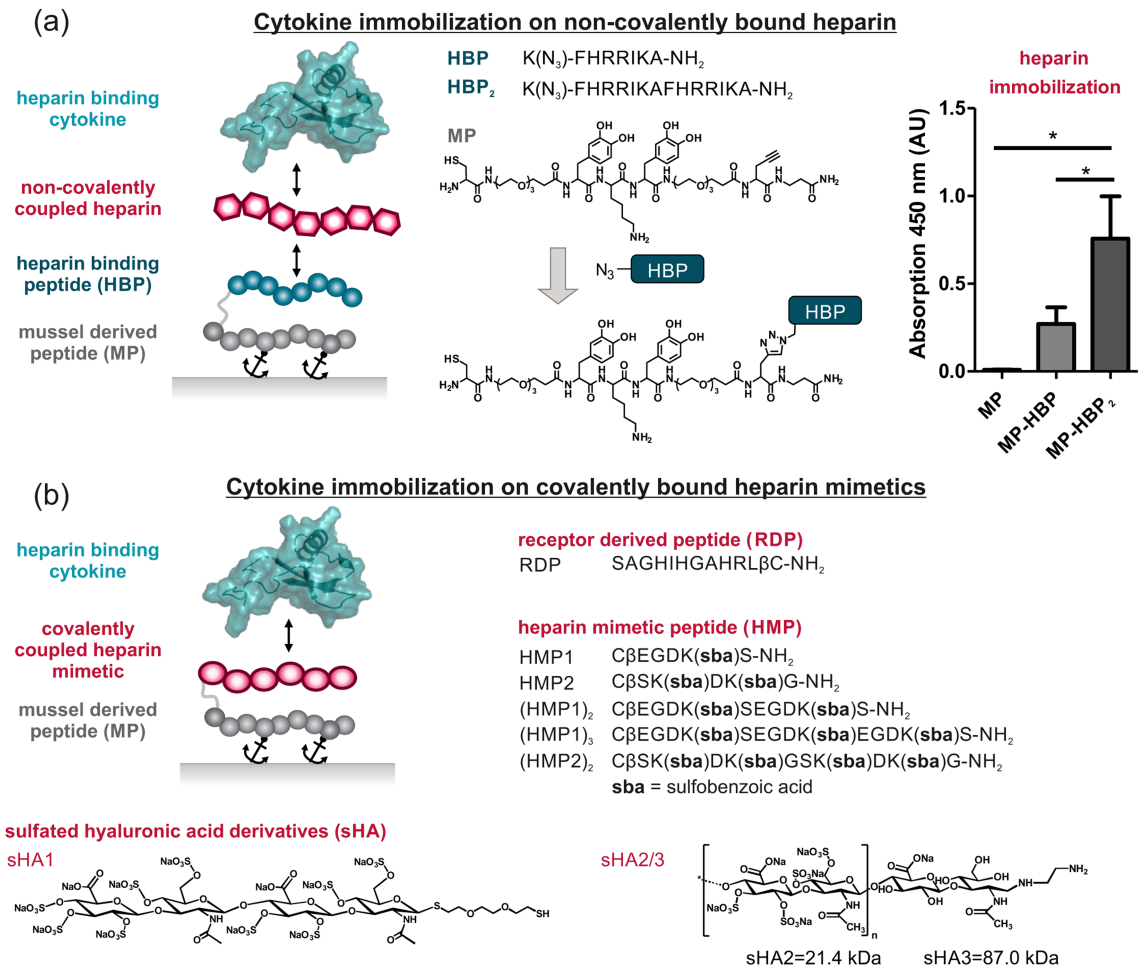

FIGURE 2 Binding and release strategies for cytokine delivery. (a) Heparin-binding peptides (HBP) enable the non-covalent immobilization of heparin and subsequent coating with cytokines. Although the peptide remains anchored to the surface, heparin and the cytokine are both released. Sequences of HBP and schematic representation of the conjugation to the mussel-derived peptide (MP) by CuAAC (middle); Heparin binding to immobilized MP-HBP and MP-HBP$_2$ as investigated in a biotin ELISA-like assay (right). $n \geq 3$, $^{*}p \leq 0.05$. (b) Covalently coupled heparin-mimetic agents release only the immobilized cytokine. Sequences of sulfated heparin-mimetic peptides (HMPs) and a CXCR4 receptor-derived peptide (RDP; right). Structures of the short persulfated hyaluronic acid derivative sHA1 (M_W = 1.902 kDa, D_S = 5.5) and higher molecular weight sulfated hyaluronic acid derivatives sHA2/3 (sHA2: M_W = 21.4 kDa, D_S = 3.5; sHA3: M_W = 87.0 kDa, D_S = 3.4; bottom). K(N_3), ε-azido-L-lysine; CuAAC, Cu(I)-catalyzed azide-alkyne cycloaddition; β, L-β-alanine; sba, 4-sulfobenzoic acid; Ac, acetate [Colour figure can be viewed at wileyonlinelibrary.com]

was detected, although the peptide was about 50-fold enriched when a preincubation with XLINK had occurred (Figure 4b).

3.3 | High CXCL12 surface loading and subsequent cell migration achieved with HBP-heparin-complexes

For investigation of CXCL12 binding, the different MP-conjugates were immobilized onto 96-well plates, and heparin-binding conjugates were additionally loaded with heparin. Subsequently, 1 μM CXCL12 was incubated on all surfaces, and retained protein was detected by specific antibodies (Figure 5a). With respect to unfunctionalized MP, five coatings were identified for CXCL12 binding: MP-RDP, MP-XLINK-sHA2, MP-XLINK-sHA3, MP-HBP-heparin, and MP-HBP$_2$-heparin. Herein, significantly higher amounts of protein were retained using the heparin binding approach. Within this scope, increased heparin affinity by sequence elongation (HBP$_2$) enhanced CXCL12 binding by two-fold. Next, we examined whether the CXCL12-binding coatings were able to induce migration in Jurkat cells, as chemotactic gradient formation and the recruitment of hematopoietic stem cells are key functions of CXCL12 (Figure 5b). However, only coatings with higher chemokine loading were able to exceed the threshold for migration induction in CXCR4-expressing cells. This was accomplished by both MP-HBP-heparin-complexes, which recruited around 15% of the cells and were on par with the positive control. However, there were no differences detectable between MP-HBP and MP-HBP$_2$ even though CXCL12 loading was twice as high on the latter.

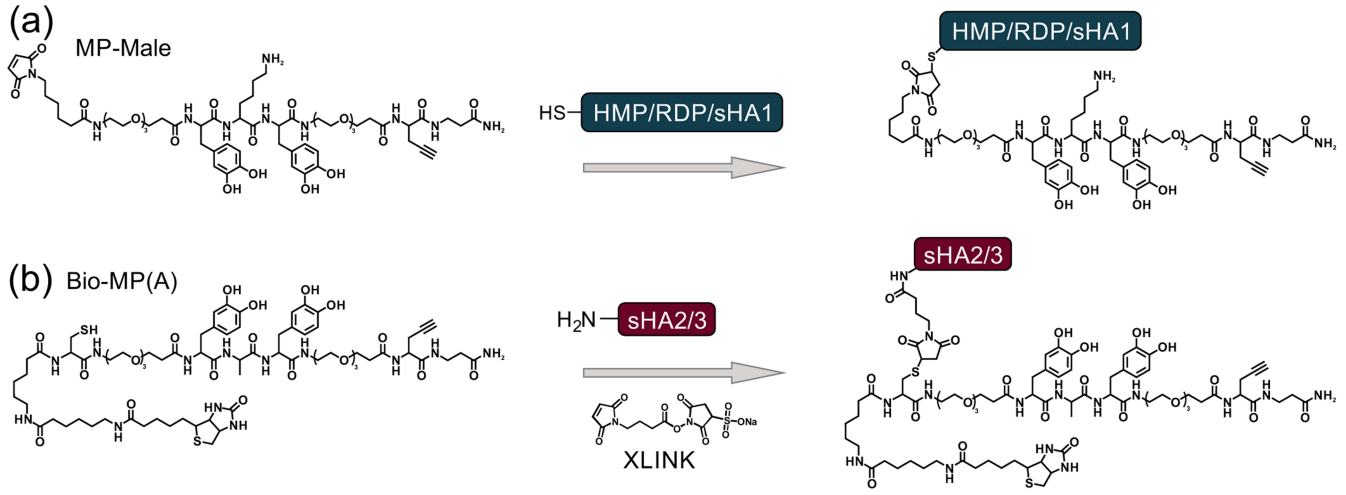

FIGURE 3 Schematic representation of the conjugation of heparin-mimetic compounds to mussel-derived peptide (MP). (a) Conjugation of heparin-mimetic peptide (HMP), receptor-derived peptide (RDP), and sHA1 via Michael addition of a thiol to an N-terminal maleimide group. (b) Conjugation of sHA2/3 to the N-terminal cysteine using a sulfo-N-succinimidyl 4-maleimidobutyrate (XLINK) crosslinker [Colour figure can be viewed at wileyonlinelibrary.com]

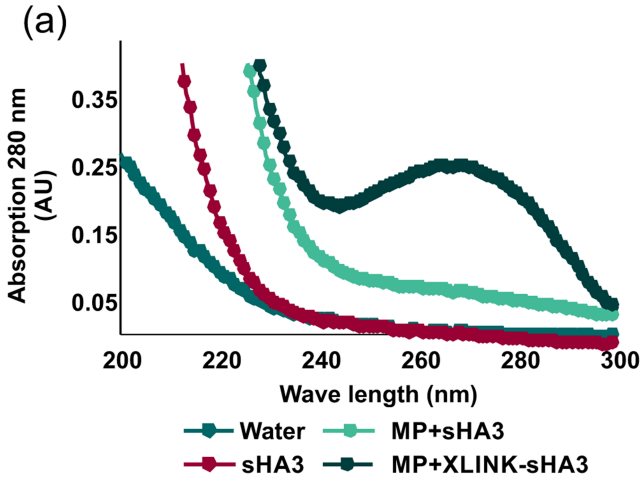

(b)

Peptide content

Peptide concentration (μM)	MP + sHA3	MP + XLINK-sHA3
	1.6	77.7
ratio		47.8

FIGURE 4 (a) Absorption scan of mussel-derived peptide (MP) and sHA3, incubated with and without crosslinker. Water and sHA3 alone served as negative controls. (b) Peptide content prior to purification by biotin-avidin affinity chromatography as determined via absorption at 280 nm [Colour figure can be viewed at wileyonlinelibrary.com]

4 | DISCUSSION

Therapeutic chemokine delivery in wound healing can be achieved in different ways. The respective chemokine can be incorporated into hydrogels and be released upon slow degradation of the biomaterial (Baumann et al., 2012). Also, it can be immobilized covalently on a solid support using an enzyme-cleavable linker mediating release by proteolytic attack (Steinhagen et al., 2014). In contrast to that, we have developed a modular peptide system consisting of a surface binding peptide that can be decorated with different cell recruiting moieties using bioorthogonal reactions (Clauder et al., 2019; Pagel et al., 2016). The advantage apart from being modular is that the peptide components are build up by solid-phase peptide synthesis allowing site-selective incorporation of nonnatural amino acids and nonamino acid components as well as full control over identity and homogeneity of the final product using standard RP-HPLC and mass spectrometry. In this study, we aimed to apply this approach in order to create a prospective delivery system for CXCL12 using affinity-based immobilization of the chemokine. Our focus was not only based on the final outcome of CXCL12 release but also on the feasibility of the production of the release system. This led us to the design, on the one hand, of a peptide carrying covalently attached heparin mimicking moieties and, on the other hand, heparin-binding peptides allowing for non-covalent immobilization of heparin followed by chemokine binding. These approaches enabled purification by RP-HPLC and identification by mass spectrometry without the need of any further verification of product homogeneity.

A prerequisite for the stable immobilization of CXCL12-binding coatings is a strong surface anchoring. This can be achieved by a bioinspired approach adapted from mussels, which adhere to virtually all kinds of substrates even in high tide and strong waves. A derived peptide coating was now shown to bind to standard PS 96-well plates, which is convenient for fundamental investigations and high-throughput studies. Binding affinity studies demonstrated a 20-fold lower EC_{50} for the DOPA-containing peptide in comparison with the tyrosine-containing control. For PS surfaces, this can be rationalized by a combination of hydrophobic, cation–π, and π–π stacking interactions (Lu et al., 2013). Although π–π stacking is based on interactions between the aromatic groups of the MP and the phenyl groups of the PS, OH–π interactions might additionally strengthen the binding and explain the observed differences between the DOPA- and the tyrosine-containing peptide (Wang & Xie, 2010). The

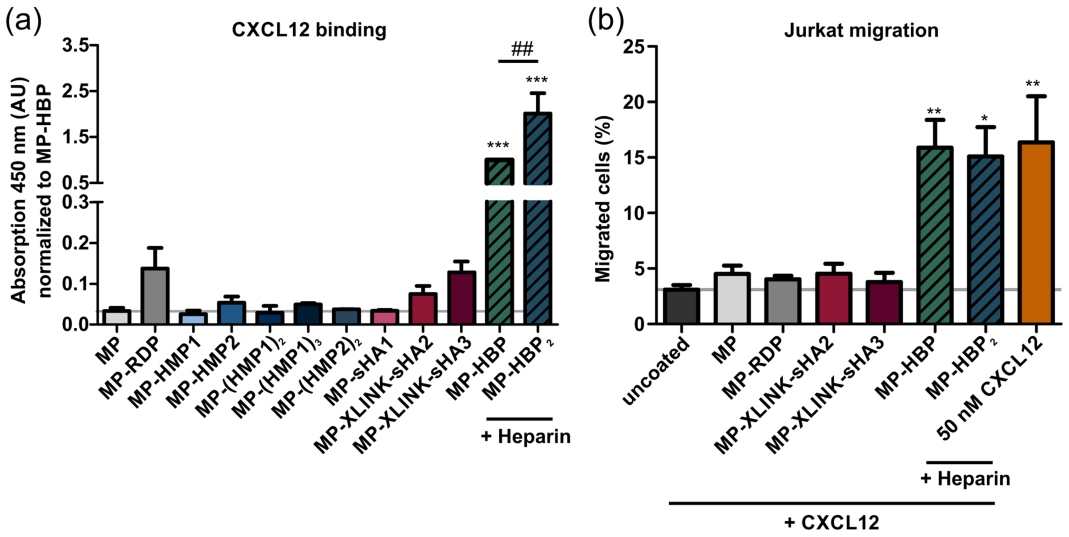

FIGURE 5 (a) CXCL12 binding to immobilized heparin-mimetic compounds (HMP), a receptor-derived peptide (RDP), and heparin-loaded heparin-binding peptides (HBP) as determined by ELISA. $n \geq 2$, *** represents significance to MP, $p \leq 0.001$; $^{\#\#}$ represents significance to MP-HBP, $p \leq 0.01$. (b) Jurkat migration toward mussel-derived peptide coatings. The lower compartments of a transwell plate were coated with peptide (+heparin) and CXCL12, whereas cells were seeded into the upper chambers. After 2 h incubation, the number of migrated cells was evaluated. Medium containing 50 nM CXCL12 served as positive control. $n \geq 3$, significance to uncoated, $^{*}p \leq 0.05$, $^{**}p \leq 0.01$ [Colour figure can be viewed at wileyonlinelibrary.com]

positively charged lysine residue provides additional binding properties via cation–π interactions and helps to abstract the hydration layer, enabling a tight binding of DOPA to the surface and limiting its oxidation (Maier, Rapp, Waite, Israelachvili, & Butler, 2015).

We then equipped MP with HBPs. Reported literature suggests that these peptides electrostatically interact with the negatively charged sulfate and carboxyl groups of heparin via the basic amino acids histidine, arginine, and lysine (Cardin & Weintraub, 1989). This was demonstrated for MP-HBP, and it is assumed that elongation of this sequence increases possible interaction sites and therefore retains significantly more heparin on the surface, as shown for MP-HBP_2. The underlying sequence FHRRIKA is derived from the bone sialoprotein (Rezania & Healy, 1999), whereas others are based on antithrombin III or the heparin-interacting protein. Investigation of consensus sequences identified clusters of one to three basic amino acids with one or two interpolated hydrophobic residues (Cardin & Weintraub, 1989). This matches the natural binding partner heparan sulfate that displays regions of varying charge densities. For optimal GAG binding, basic and hydrophobic residues should likewise alternate (Fromm, Hileman, Caldwell, Weiler, & Linhardt, 1995). In addition, the secondary structure also needs to be taken into consideration, as heparin binding can induce conformational changes and align the basic residues in spatial proximity facing the GAG (Capila & Linhardt, 2002).

Subsequently, CXCL12 binding was confirmed on the peptide-heparin-complexes. Notably, the higher heparin-binding capacity of MP-HBP_2 also retained significantly more CXCL12 in comparison with MP-HBP. Tight packing of the small peptides on the surface and high loading with heparin might be an explanation. Surprisingly, both coatings proved to be equal, when studying cell recruitment in a transwell assay. However, chemoattraction works in a broad range of concentrations as cells are able to compare signals reaching front and rear of the membrane, possess the ability to amplify detected differences, and perform background subtraction of uniform receptor-occupancy (Kutscher, Devreotes, & Iglesias, 2004). Another reason for the unexpected indifference between the two coatings could lie within the heparin sequestration. In addition to higher amounts of chemokine, more heparin is simultaneously released from MP-HBP_2. Even though GAG and receptor-binding sites are clearly separated in CXCL12 and the protein remains active in a complex (Laguri, Arenzana-Seisdedos, & Lortat-Jacob, 2008; Sweeney, Lortat-Jacob, Priestley, Nakamoto, & Papayannopoulou, 2002), soluble heparin might act as a scavenger for membrane clustering. Cell-surface proteoglycans locally enhance CXCL12 concentration toward the receptor, and free heparin would compete with their interaction, disconnecting the chemokine from the receptor binding site (Kuschert et al., 1999).

In comparison with the modular approach using non-covalently immobilized heparin for cytokine release, direct functionalization of MP with heparin-mimetic compounds was investigated. Herein, only the cytokine, but not the electrostatically bound heparin, would be released into the surrounding tissues over time. Even though heparin is extensively used as an anticoagulant, it is associated with a number of adverse effects (Gervin, 1975). In addition, the pharmaceutical production of heparin still solely relies on animal tissue. The process is highly optimized and cost-effective, but quality control is difficult and the risk of adulteration and contamination remains (Oduah, Linhardt, & Sharfstein, 2016). Potential shortages resulting from a strong dependency on porcine heparin mainly produced in China as well as animal rights and environmental concerns demand alternative manufacturing processes (Fu, Suflita, & Linhardt, 2016). Synthetic analogs might provide a solution and are subject to extensive research. Even though the

production can be laborious and hard to upscale, they provide better control and higher chemical versatility for the incorporation into functional materials. Therefore, we considered synthetic peptides as well as HA derivatives as heparin mimetics for the covalent coupling to MP. Previous reports had demonstrated that anionic charges solely derived from hydroxyl and carboxyl groups are insufficient to retain CXCL12, as demonstrated for HA in an NMR study (Panitz et al., 2016). Consequentially, sulfated derivatives were produced.

However, HMP coatings were generally less efficient in CXCL12 binding. None of the sulfated peptides were able to accumulate CXCL12, neither as single nor as double or triple motif, respectively. This was unexpected, as the HMPs in principle display the three functional groups of heparin—sulfates, carboxylates, and hydroxyl groups and were confirmed to bind various cytokines in preceding studies (Hendrikse et al., 2018; Mammadov et al., 2012; Maynard & Hubbell, 2005). However, in these approaches, the peptides are presented in a three-dimensional arrangement on self-assembled nanofibers in contrast to our two-dimensional surface modification. For the hyaluronan-based coatings, a length-dependent effect is observed. The short tetrasaccharide in MP-sHA1 was insufficient for immobilizing CXCL12, whereas the longer variants retained at least small amounts of the protein. In principle, the chemokine CXCL12 dimerizes upon heparin binding (Fermas et al., 2008) and subsequently displays two distinct GAG-binding sites. The main binding site, so called high-affinity heparin-binding region, is located at the dimer interface, where a number of basic residues create a positively charged crevice (Sadir, Baleux, Grosdidier, Imberty, & Lortat-Jacob, 2001). Residues of the consensus sequence BBXB in the first β-strand (Lys24, His25, and Lys27; Amara et al., 1999) as well as spatially adjacent Arg41 and Lys43 (Sadir et al., 2001) were found to play a major role. The second binding site, called low-affinity heparin-binding region, includes the N-terminal loop and the α-helix. Important residues involved in this interaction include Arg20, Ala21, Asn30, and Lys64 (Murphy et al., 2007). To span the high-affinity heparin binding region, 12 to 14 monosaccharide units are required (Sadir et al., 2001). The small sulfopeptides and the tetrasaccharide are probably too short to efficiently interact with CXCL12. However, sequence elongation of the sulfated peptides did not enhance the protein-binding capacity, which suggests that the defined pattern of carboxyl and sulfate groups in heparan sulfate is not met correctly. Studies show that especially 2-O- and N-sulfate groups contribute to CXCL12 binding (Sadir et al., 2001) as well as 6-O-sulfation to a lesser extent (Zhang et al., 2012). Also, L-iduronic acid provides conformational flexibility that is believed to be responsible for the variety of proteins that can be bound specifically (Mulloy & Forster, 2000). For the HMPs, the sulfate groups might not be displayed in the correct conformation with respect to orientation, spacing, and distance from the peptide backbone, as a rather long linker was introduced by using sba. Although heparan sulfate is only moderately sulfated with an average of one sulfate group per disaccharide, heparin is highly sulfated with an average of 2.7 sulfate groups per disaccharide. In comparison, the degree of sulfation of the tetrasaccharide is still much higher, with 4.5 sulfate groups per disaccharide, which could also be a disadvantage for the interaction. On the other hand, the difference to heparin is not as big for the higher molecular weight HA derivatives, which display 3.5 (sHA2) and 3.4 sulfate groups (sHA3), respectively. However, N-sulfation is completely absent in all of these compounds. When comparing the glycosidic linkage, the monomers of the HA derivatives are (1 → 3)–linked and in the disaccharides (1 → 4), whereas in heparin and heparan sulfates, both units are (1 → 4)–linked. This additionally contributes to a discrepant arrangement of the sulfation pattern.

Taken together, the two-step coating protocol using HBPs and electrostatically bound heparin was most efficient in immobilizing the chemokine CXCL12 and recruiting cells to coated surfaces. This was rationalized by a high binding affinity toward the cytokine, owing to an unaltered charge display of the incorporated natural heparin. In addition, small HBP coatings can be prepared in a relatively easy fashion using solid-phase peptide synthesis and bioorthogonal reactions followed by simple RP-HPLC purification. As seen for sHA2 and sHA3, using larger GAGs for covalent immobilization requires more sophisticated purification protocols, and there still remains uncertainty on the homogeneity and consistent functionality of the final product. Also, HBPs reach high surface packings and are uncomplicated and more stable to pH changes during synthesis. By alteration of the HBP, the amount of heparin and heparin-binding cytokines can be tuned, catering to therapeutic purposes.

5 | CONCLUSION

In our study, a two-layer approach, where immobilized HBPs are subsequently loaded with heparin, was identified to be the best condition for a prospective chemokine delivery system, as the highest amount of CXCL12 was bound and the strongest effects on cell migration were detected. However, maintaining the balance between chemokine and codelivered heparin is crucial to success and multiple factors involving scavenging effects, side reactivity, and supply ethics need to be taken into consideration. Even though the synthetic compounds tested in this study could not compete with the natural product, extensive progress has been made in carbohydrate chemistry within the past years, and the development of compounds displaying the appropriate interaction sites for chemokine binding are subject to the near future (Mohamed & Coombe, 2017). This will have many benefits, as synthetic compounds provide higher structural control and allow fine-tuning of the protein binding affinity. One might imagine the creation of a more stable gradient by modulating the strength of the affinity interactions (Vulic & Shoichet, 2014), either the GAG component with higher or lower protein-binding affinities or engineered proteins displaying a stronger or weaker GAG-binding affinity (Spiller et al., 2019). In both cases, mussel-derived surface-binding peptides provide a versatile platform that is additionally modifiable with other bioactive peptides. Combinations of cell adhesion and HBPs can cooperatively enhance tissue regeneration (Pagel et al., 2016) and provide a huge toolbox customizable to the specific needs of future applications.

ACKNOWLEDGEMENTS

We thankfully acknowledge Dr. Katharina Lemmnitzer and Dr. Jürgen Schiller for assistance in mass spectrometry of sulfated GAG derivatives. Moreover, Kristin Löbner, Regina Reppich-Sacher, Ronny Müller, and Martin Striegler are thanked for technical assistance during cell culture and synthesis. We express our thanks to the Deutsche Forschungsgemeinschaft (TR67, A04, A08, and Z03), the European Union and the Free State of Saxony, the Helmholtz-Institute for Metabolism, Adipositas and Vascular Research (HI-MAG), and the Research Academy Leipzig for financial support. Open access funding enabled and organized by Projekt DEAL.

AUTHOR CONTRIBUTIONS

Author contribution are as follows: design, data collection and interpretation, and manuscript drafting (F. C.); synthesis and analysis of sHA2/3 and manuscript drafting (S. M.); synthesis and analysis of sHA1 and manuscript drafting (S. K.); pH-dependent heparin-binding studies, data interpretation, and drafting of revision (K. B. S.); supervision of synthesis sHA1 and manuscript revision (J. R.); supervision of synthesis sHA2/3 and manuscript revision (M. S.); design, data interpretation, manuscript drafting, and revision (A. B. S.). All authors have approved the final version of the manuscript. All authors have agreed to be accountable for all aspects of the work in ensuring that questions related to the accuracy or integrity of any part of the work are appropriately investigated and resolved.

CONFLICTS OF INTEREST

The authors declare no conflict of interest.

ORCID

Kathrin Bellmann-Sickert https://orcid.org/0000-0002-0007-008X
Jörg Rademann https://orcid.org/0000-0001-6678-3165
Annette G. Beck-Sickinger https://orcid.org/0000-0003-4560-8020

REFERENCES

Amara, A., Lorthioir, O., Valenzuela, A., Magerus, A., Thelen, M., Montes, M., … Arenzana-Seisdedos, F. (1999). Stromal cell-derived factor-1alpha associates with heparan sulfates through the first beta-strand of the chemokine. *The Journal of Biological Chemistry*, *274*(34), 23916–23925. https://doi.org/10.1074/jbc.274.34.23916

Baumann, L., Prokoph, S., Gabriel, C., Freudenberg, U., Werner, C., & Beck-Sickinger, A. G. (2012). A novel, biased-like SDF-1 derivative acts synergistically with starPEG-based heparin hydrogels and improves eEPC migration in vitro. *Journal of Controlled Release: Official Journal of the Controlled Release Society*, *162*(1), 68–75. https://doi.org/10.1016/j.jconrel.2012.04.049

Capila, I., & Linhardt, R. J. (2002). Heparin-protein interactions. *Angewandte Chemie*, *41*(3), 391–412. https://doi.org/10.1002/1521-3773(20020201)41:3<390::aid-anie390>3.0.co;2-b

Cardin, A. D., & Weintraub, H. J. (1989). Molecular modeling of protein-glycosaminoglycan interactions. *Arteriosclerosis*, *9*(1), 21–32. https://doi.org/10.1161/01.atv.9.1.21

Clauder, F., Czerniak, A. S., Friebe, S., Mayr, S. G., Scheinert, D., & Beck-Sickinger, A. G. (2019). Endothelialization of titanium surfaces by bioinspired cell adhesion peptide coatings. *Bioconjugate Chemistry*, *30*(10), 2664–2674. https://doi.org/10.1021/acs.bioconjchem.9b00573

Fermas, S., Gonnet, F., Sutton, A., Charnaux, N., Mulloy, B., Du, Y., … Daniel, R. (2008). Sulfated oligosaccharides (heparin and fucoidan) binding and dimerization of stromal cell-derived factor-1 (SDF-1/CXCL 12) are coupled as evidenced by affinity CE-MS analysis. *Glycobiology*, *18*(12), 1054–1064. https://doi.org/10.1093/glycob/cwn088

Fromm, J. R., Hileman, R. E., Caldwell, E. E., Weiler, J. M., & Linhardt, R. J. (1995). Differences in the interaction of heparin with arginine and lysine and the importance of these basic amino acids in the binding of heparin to acidic fibroblast growth factor. *Archives of Biochemistry and Biophysics*, *323*(2), 279–287. https://doi.org/10.1006/abbi.1995.9963

Fu, L., Suflita, M., & Linhardt, R. J. (2016). Bioengineered heparins and heparan sulfates. *Advanced Drug Delivery Reviews*, *97*, 237–249. https://doi.org/10.1016/j.addr.2015.11.002

Gervin, A. S. (1975). Complications of heparin therapy. *Surgery, Gynecology & Obstetrics*, *140*(5), 789–796.

Guyon, A. (2014). CXCL12 chemokine and its receptors as major players in the interactions between immune and nervous systems. *Frontiers in Cellular Neuroscience*, *8*, 65. https://doi.org/10.3389/fncel.2014.00065

Hassert, R., Pagel, M., Ming, Z., Haupl, T., Abel, B., Braun, K., … Beck-Sickinger, A. G. (2012). Biocompatible silicon surfaces through orthogonal click chemistries and a high affinity silicon oxide binding peptide. *Bioconjugate Chemistry*, *23*(10), 2129–2137. https://doi.org/10.1021/bc3003875

Hendrikse, S. I. S., Spaans, S., Meijer, E. W., & Dankers, P. Y. W. (2018). Supramolecular platform stabilizing growth factors. *Biomacromolecules*, *19*(7), 2610–2617. https://doi.org/10.1021/acs.biomac.8b00219

Janssens, R., Struyf, S., & Proost, P. (2018). The unique structural and functional features of CXCL12. *Cellular & Molecular Immunology*, *15*(4), 299–311. https://doi.org/10.1038/cmi.2017.107

Ji, W., Yang, F., Ma, J., Bouma, M. J., Boerman, O. C., Chen, Z., … Jansen, J. A. (2013). Incorporation of stromal cell-derived factor-1alpha in PCL/gelatin electrospun membranes for guided bone regeneration. *Biomaterials*, *34*(3), 735–745. https://doi.org/10.1016/j.biomaterials.2012.10.016

Köhling, S., Blaszkiewicz, J., Ruiz-Gomez, G., Fernandez-Bachiller, M. I., Lemmnitzer, K., Panitz, N., … Rademann, J. (2019). Syntheses of defined sulfated oligohyaluronans reveal structural effects, diversity and thermodynamics of GAG-protein binding. *Chemical Science*, *10*(3), 866–878. https://doi.org/10.1039/c8sc03649g

Kunze, R., Rosler, M., Möller, S., Schnabelrauch, M., Riemer, T., Hempel, U., & Dieter, P. (2010). Sulfated hyaluronan derivatives reduce the proliferation rate of primary rat calvarial osteoblasts. *Glycoconjugate Journal*, *27*(1), 151–158. https://doi.org/10.1007/s10719-009-9270-9

Kuschert, G. S., Coulin, F., Power, C. A., Proudfoot, A. E., Hubbard, R. E., Hoogewerf, A. J., & Wells, T. N. (1999). Glycosaminoglycans interact selectively with chemokines and modulate receptor binding and cellular responses. *Biochemistry*, *38*(39), 12959–12968. https://doi.org/10.1021/bi990711d

Kutscher, B., Devreotes, P., & Iglesias, P. A. (2004). Local excitation, global inhibition mechanism for gradient sensing: An interactive applet. *Science's STKE: Signal Transduction Knowledge Environment*, *2004*(219), pl3. https://doi.org/10.1126/stke.2192004pl3

Laguri, C., Arenzana-Seisdedos, F., & Lortat-Jacob, H. (2008). Relationships between glycosaminoglycan and receptor binding sites in chemokines-the CXCL12 example. *Carbohydrate Research*, *343*(12), 2018–2023. https://doi.org/10.1016/j.carres.2008.01.047

Liekens, S., Schols, D., & Hatse, S. (2010). CXCL12-CXCR4 axis in angiogenesis, metastasis and stem cell mobilization. *Current Pharmaceutical Design*, *16*(35), 3903–3920. https://doi.org/10.2174/138161210794455003

Lu, Q., Danner, E., Waite, J. H., Israelachvili, J. N., Zeng, H., & Hwang, D. S. (2013). Adhesion of mussel foot proteins to different substrate

surfaces. *Journal of the Royal Society, Interface*, *10*(79), 20120759. https://doi.org/10.1098/rsif.2012.0759

Maier, G. P., Rapp, M. V., Waite, J. H., Israelachvili, J. N., & Butler, A. (2015). Adaptive synergy between catechol and lysine promotes wet adhesion by surface salt displacement. *Science*, *349*(6248), 628–632. https://doi.org/10.1126/science.aab0556

Mammadov, R., Mammadov, B., Guler, M. O., & Tekinay, A. B. (2012). Growth factor binding on heparin mimetic peptide nanofibers. *Biomacromolecules*, *13*(10), 3311–3319. https://doi.org/10.1021/bm3010897

Mammadov, R., Mammadov, B., Toksoz, S., Aydin, B., Yagci, R., Tekinay, A. B., & Guler, M. O. (2011). Heparin mimetic peptide nanofibers promote angiogenesis. *Biomacromolecules*, *12*(10), 3508–3519. https://doi.org/10.1021/bm200957s

Maynard, H. D., & Hubbell, J. A. (2005). Discovery of a sulfated tetrapeptide that binds to vascular endothelial growth factor. *Acta Biomaterialia*, *1*(4), 451–459. https://doi.org/10.1016/j.actbio.2005.04.004

Mohamed, S., & Coombe, D. R. (2017). Heparin mimetics: Their therapeutic potential. *Pharmaceuticals*, *10*(4). https://doi.org/10.3390/ph10040078

Mulloy, B., & Forster, M. J. (2000). Conformation and dynamics of heparin and heparan sulfate. *Glycobiology*, *10*(11), 1147–1156. https://doi.org/10.1093/glycob/10.11.1147

Murphy, J. W., Cho, Y., Sachpatzidis, A., Fan, C., Hodsdon, M. E., & Lolis, E. (2007). Structural and functional basis of CXCL12 (stromal cell-derived factor-1 alpha) binding to heparin. *The Journal of Biological Chemistry*, *282*(13), 10018–10027. https://doi.org/10.1074/jbc.M608796200

Oduah, E. I., Linhardt, R. J., & Sharfstein, S. T. (2016). Heparin: Past, present, and future. *Pharmaceuticals*, *9*(3). https://doi.org/10.3390/ph9030038

Pagel, M., Hassert, R., John, T., Braun, K., Wiessler, M., Abel, B., & Beck-Sickinger, A. G. (2016). Multifunctional coating improves cell adhesion on titanium by using cooperatively acting peptides. *Angewandte Chemie*, *55*(15), 4826–4830. https://doi.org/10.1002/anie.201511781

Panitz, N., Theisgen, S., Samsonov, S. A., Gehrcke, J. P., Baumann, L., Bellmann-Sickert, K., … Beck-Sickinger, A. G. (2016). The structural investigation of glycosaminoglycan binding to CXCL12 displays distinct interaction sites. *Glycobiology*, *26*(11), 1209–1221. https://doi.org/10.1093/glycob/cww059

Peled, A., Eizenberg, O., & Vaizel-Ohayon, D. (2012). US Patent No. 274.478. Washington, DC: U. P. a. T. Office.

Purcell, B. P., Kim, I. L., Chuo, V., Guinen, T., Dorsey, S. M., & Burdick, J. A. (2014). Incorporation of sulfated hyaluronic acid macromers into degradable hydrogel scaffolds for sustained molecule delivery. *Biomaterials Science*, *2*, 693–702. https://doi.org/10.1039/C3BM60227C

Ratajczak, M. Z., Zuba-Surma, E., Kucia, M., Reca, R., Wojakowski, W., & Ratajczak, J. (2006). The pleiotropic effects of the SDF-1-CXCR4 axis in organogenesis, regeneration and tumorigenesis. *Leukemia*, *20*(11), 1915–1924. https://doi.org/10.1038/sj.leu.2404357

Rezania, A., & Healy, K. E. (1999). Biomimetic peptide surfaces that regulate adhesion, spreading, cytoskeletal organization, and mineralization of the matrix deposited by osteoblast-like cells. *Biotechnology Progress*, *15*(1), 19–32. https://doi.org/10.1021/bp980083b

Sadir, R., Baleux, F., Grosdidier, A., Imberty, A., & Lortat-Jacob, H. (2001). Characterization of the stromal cell-derived factor-1alpha-heparin complex. *The Journal of Biological Chemistry*, *276*(11), 8288–8296. https://doi.org/10.1074/jbc.M008110200

Sakiyama-Elbert, S. E., & Hubbell, J. A. (2000). Controlled release of nerve growth factor from a heparin-containing fibrin-based cell ingrowth matrix. *Journal of Controlled Release: Official Journal of the Controlled Release Society*, *69*(1), 149–158. https://doi.org/10.1016/s0168-3659(00)00296-0

Spiller, S., Panitz, N., Schirmer, L., Atallah, P. M., Limasale, Y. D. P., Bellmann-Sickert, K., … Beck-Sickinger, A. G. (2019). Modulation of human CXCL12 binding properties to glycosaminoglycans to improve the chemotactic gradient. *ACS Biomaterials Science & Engineering*, *5*(10), 5128–5138. https://doi.org/10.1021/acsbiomaterials.9b01139

Steinhagen, M., Hoffmeister, P. G., Nordsieck, K., Hotzel, R., Baumann, L., Hacker, M. C., … Beck-Sickinger, A. G. (2014). Matrix metalloproteinase 9 (MMP-9) mediated release of MMP-9 resistant stromal cell-derived factor 1alpha (SDF-1alpha) from surface modified polymer films. *ACS Applied Materials & Interfaces*, *6*(8), 5891–5899. https://doi.org/10.1021/am500794q

Sweeney, E. A., Lortat-Jacob, H., Priestley, G. V., Nakamoto, B., & Papayannopoulou, T. (2002). Sulfated polysaccharides increase plasma levels of SDF-1 in monkeys and mice: Involvement in mobilization of stem/progenitor cells. *Blood*, *99*(1), 44–51. https://doi.org/10.1182/blood.v99.1.44

Tsukada, K., Tokunaga, K., Iwama, T., & Mishima, Y. (1979). The pH changes of pressure ulcers related to the healing process of wounds. *Wounds*, *1992*(4), 16–20.

Veldkamp, C. T., Seibert, C., Peterson, F. C., Sakmar, T. P., & Volkman, B. F. (2006). Recognition of a CXCR4 sulfotyrosine by the chemokine stromal cell-derived factor-1alpha (SDF-1alpha/CXCL12). *Journal of Molecular Biology*, *359*(5), 1400–1409. https://doi.org/10.1016/j.jmb.2006.04.052

Vulic, K., & Shoichet, M. S. (2014). Affinity-based drug delivery systems for tissue repair and regeneration. *Biomacromolecules*, *15*(11), 3867–3880. https://doi.org/10.1021/bm501084u

Waite, J. H., & Tanzer, M. L. (1981). Polyphenolic substance of Mytilus edulis: Novel adhesive containing L-dopa and hydroxyproline. *Science*, *212*(4498), 1038–1040. https://doi.org/10.1126/science.212.4498.1038

Wang, R., & Xie, T. (2010). Macroscopic evidence of strong cation-pi interactions in a synthetic polymer system. *Chemical Communications*, *46*(8), 1341–1343. https://doi.org/10.1039/b916204f

Wilson, I. A., Henry, M., Quill, R. D., & Byrne, P. J. (1979). The pH of varicose ulcer surfaces and its relationship to healing. *VASA. Zeitschrift Fur Gefasskrankheiten*, *8*(4), 339–342.

Zhang, S., Condac, E., Qiu, H., Jiang, J., Gutierrez-Sanchez, G., Bergmann, C., … Wang, L. (2012). Heparin-induced leukocytosis requires 6-O-sulfation and is caused by blockade of selectin- and CXCL12 protein-mediated leukocyte trafficking in mice. *The Journal of Biological Chemistry*, *287*(8), 5542–5553. https://doi.org/10.1074/jbc.M111.314716

SUPPORTING INFORMATION

Additional supporting information may be found online in the Supporting Information section at the end of this article.

Table S1. Analytical data of the synthesized precursor peptides and conjugates.

Figure S1. Heparin binding to immobilized MP-HBP and MP-HBP_2 as investigated in a biotin ELISA-like assay at different pH conditions. $n = 2$, * $p \leq 0.05$, ns = non significant.

Table S2. Analytical data of the sulfated hyaluronic acid derivatives sHA2 and sHA3.

How to cite this article: Clauder F, Möller S, Köhling S, et al. Peptide-mediated surface coatings for the release of wound-healing cytokines. *J Tissue Eng Regen Med*. 2020;14:1738–1748. https://doi.org/10.1002/term.3123